



ELSEVIER

International Journal of Mass Spectrometry 185/186/187 (1999) 825–835



Formation of some transition metal oxide cluster anions and reactivity towards methanol in the gas phase

M.C. Oliveira^a, J. Marçalo^b, M.C. Vieira^b, M.A. Almoister Ferreira^{a,c,*}

^aCentro de Espectrometria de Massa, Complexo I-IST, Av. Rovisco Pais, 1096 Lisboa Codex, Portugal

^bDepartamento de Química, Instituto Tecnológico e Nuclear, 2686 Sacavém Codex, Portugal

^cDepartamento de Química, Faculdade de Ciências, Universidade de Lisboa, Campo Grande, Ed. C1-5° Piso, 1700 Lisboa, Portugal

Received 15 July 1998; accepted 29 September 1998

Abstract

Negative cluster ions of transition metal oxides ($[M_xO_y]^-$; M = Mn, Fe, Co, Ni, Cu) have been generated by laser desorption ionisation from metal oxide pellets and studied using Fourier transform ion cyclotron resonance mass spectrometry. For the same metal, the stoichiometrically different oxides yield similar collections of anions, with small differences in the ion intensity distributions. The most intense transition metal anions were isolated and their reactivity towards methanol was investigated. The $[MO_2]^-$, $[M_2O_3]^-$ and $[M_2O_4]^-$ anions react exothermically with methanol leading to $[MO_2H_2]^-$, $[M_2O_3H_2]^-$ and $[M_2O_4H_2]^-$ as primary products, respectively. The $[MO_3]^-$ anions are unreactive towards methanol. The rate constants determined for the various reactions suggest that the $[MO_2]^-$ and $[M_2O_3]^-$ anions react more efficiently with methanol than the $[M_2O_4]^-$ cluster anions. The reaction efficiencies decrease when the metal varies from manganese to copper indicating that the number of electrons in the *d* shell of the metal atom appears to be an important factor on reactivity. (Int J Mass Spectrom 185/186/187 (1999) 825–835) © 1999 Elsevier Science B.V.

Keywords: Transition metal oxide anions; Laser desorption ionisation; Fourier transform ion cyclotron resonance mass spectrometer; Reactivity; Cluster anions

1. Introduction

Transition-metal oxides have been the subject of considerable interest because of the important role that these compounds play in a variety of processes including catalysis, corrosion, combustion, and biological systems. The study of the gas-phase chemistry of these compounds can provide information about their intrinsic chemical and physical properties and it

can contribute to a better understanding of their behaviour in the condensed phase.

Most of the investigations concerning the properties and reactivity of transition metal oxides in the gas phase refer to cationic species [1–7] although in the last years a few studies have been made of anions involving these compounds. Gaseous reactions between dioxygen and metal carbonyl anions in a flowing afterglow apparatus [8,9] and in the cell of a Fourier transform ion cyclotron resonance (FTICR) mass spectrometer [9,10] were used to generate several oxometallate anions of the first and second transition metal series. Negatively charged oxides of

* Corresponding author.

Dedicated to Professor Michael T. Bowers on the occasion of his 60th birthday.

Groups 5 and 6 were produced by vaporisation from a heated filament in a fast-flow reactor and their properties and reactivity with several substrates were investigated [11]. Molybdenum oxide cluster anions have also been produced from a filament source and its reactions with O₂, NO, and NO₂ were studied in a fast flow apparatus [12]. Cationic and anionic [FeO₂] species were generated by chemical ionisation of a mixture of Fe(CO)₅ and O₂ and the connectivities of the ions were probed by various mass spectrometric methods [13]. The direct laser vaporisation has been a successful approach to the generation of metal oxide cluster ions. Michiels and Gijbels [14,15] have used laser microprobe mass analysis (LAMMA) for the characterisation of binary oxides of metals belonging to different groups in the Periodic Table. Freiser and co-workers [16] generated positive and negative copper oxide clusters by direct laser desorption ionisation of copper oxide pellets and collisional induced dissociations of these ions were carried out in a FTICR mass spectrometer in order to discuss their stabilities. Direct laser vaporisation and fast atom bombardment (FAB) coupled with FTICR mass spectrometry have been employed to study the formation and fragmentation of molybdenum oxide cluster ions [Mo_xO_y][±] [17]. Cluster ions formed from powdered chromium oxides and salts have been examined by time-of-flight laser microprobe mass spectrometry (TOF-LMMS) and by FTICR mass spectrometry and the experimental results compared with density functional theoretical calculations [18]. A systematic study of iron oxide molecules involving one or two iron atoms [19,20] and of small copper oxide clusters [21,22] using anion photoelectron spectroscopy provided useful information about the chemical bonding and structures of these molecules. Recently, Castleman and co-workers [23] used a fast flow reactor quadrupole mass spectrometer coupled with a laser vaporisation source to study the gas phase reactions of nickel oxide cluster anions with nitric oxide. Also, studies of “molecular speciation” of inorganic analytes including some transition metal oxides by FT-LMMS yielded detailed information of local constituents at the surface of solids [24,25]. It was found that the cluster ion

compositions reflected the molecular composition of the analyte in a specific and systematic way.

In the present study, laser desorption ionisation (LDI) coupled with FTICR mass spectrometry has been employed to generate and characterise transition-metal oxide anions ([M_xO_y][−]; M = Mn, Fe, Co, Ni, Cu) using metal oxide powders as starting material. To investigate the influence of the composition and structure of the solid sample on the ions produced by LDI, metal oxides of different stoichiometries were analysed as well as one mixed-metal oxide and a physical mixture of two pure metal oxides. To obtain information on the stability and structure of the metal oxide anions collisional induced dissociation experiments were performed, and the reactivity of the more abundant [M_xO_y][−] ions with methanol and D-labelled methanol were investigated.

2. Experimental

The experiments were performed on a Finnigan FT/MS 2001-DT FTICR mass spectrometer equipped with a 3 tesla superconducting magnet and interfaced with a Spectra-Physics Quanta-Ray GCR-11 Nd:YAG laser operated at the fundamental wavelength (1064 nm). The cluster anions were generated by direct laser desorption ionisation of transition metal oxide pellets mounted on the automatic solids probe near the front trapping plate of the source side of the dual cell where the Nd:YAG laser was focused. The laser was Q switched to produce a 2.5 ns pulse duration and the laser power was varied between 45 and 60 mJ per pulse.

Pure metal oxide pellets were prepared from commercially available powders (Aldrich). The mixed-metal oxide (NiCo₂O₄) pellet was prepared from a synthesised sample [26] and a 1.5:1 (w/w) mixture of pure metal oxides powders, NiO and Co₃O₄ was also analysed.

After formation and trapping of the [M_xO_y][−] anions, the anion for study was isolated using the SWIFT method [27], a computer controlled protocol for ion excitation and ejection in the FTICR experimental event sequence, and its ion/molecule reactions

with CH₃OH and CD₃OD were investigated. The methanol and *D*-labelled alcohols were introduced in the spectrometer through a leak valve, to obtain pressures in the range of 7×10^{-8} to 5×10^{-7} Torr on the “source” side of the dual ion trap of the instrument, as measured by a calibrated ion gauge placed away from the cell [28]. Before performing the experiments with *D*-labelled alcohols, electron impact mass spectra of the substrates were recorded in order to determine the degree of labelling inside the cell. It was observed that some CH₃OH and CD₃OH were indeed present but with lower abundances than CH₃OD and CD₃OD, about 40% and 15%, respectively. Rate constants were determined by observing the pseudo-first order decay of the reactant ion relative intensity as a function of time at constant reagent pressure. Reaction efficiencies are reported as fractions of the theoretical collisional rates, k_{ADO} , using the average dipole orientation (ADO) theory [29] and experimental values of dipole moment and polarizability of methanol [30]. Uncertainties in the pressure calibration procedure may lead to errors in the absolute rate constants that we estimate to be $\pm 50\%$, but the relative magnitudes of the reaction efficiencies should have errors lower than 20%.

In order to remove possible excess of internal/translational energy of the reactant $[\text{M}_x\text{O}_y]^-$ anions prior to their reactions with the substrate, thermalisation was performed. It typically involved 1 s collisional cooling periods after the introduction of argon into the vacuum chamber through pulsed solenoid valves to maximum pressures of the order of 10^{-5} Torr.

High resolution measurements and the experiments with deuterated methanol were used to assign the composition of the cluster ions and of the ionic products formed on the ion-molecule reactions. The reaction sequences were confirmed with double-resonance experiments, in which suppression of the daughter ion is sought by ejection of the supposed parent.

In order to obtain structural information, collision-induced dissociation (CID) experiments were performed by translational excitation of the ion of interest with a rf pulse to laboratory frame energies in the

ranging of 20–100 eV in the presence of an inert target gas such as argon at the pressure of about 10^{-6} Torr.

3. Results and discussion

3.1. Formation of cluster anions

The laser desorption ionisation mass spectra of MnO, MnO₂, Mn₂O₃, Mn₃O₄, Fe₂O₃, Fe₃O₄, Co₃O₄, NiO, CuO, and Cu₂O pellets show an abundant number of negative cluster ions. Fig. 1 shows a broadband mass spectrum of the cobalt oxide. In general, the most intense anion peaks occur in the lower-mass range of the spectra, and a rapid decrease of cluster ion intensity was observed with increasing size. For the same metal, the stoichiometrically different oxides yield similar collections of anions, with small differences in the ion intensity distributions.

The correlation between the ion distributions, their abundances and the stoichiometry of the compounds has been discussed by several groups. Willet and co-workers [31–34] used laser ablation coupled with FTICR mass spectrometry to generate and characterise a large number of metal sulfide clusters. They observed that in general the distribution of ions $[\text{M}_x\text{S}_y]^-$ and their relative abundances were largely independent of the composition of the solid precursor used in the laser ablation. On the other hand, Michiels and Gijbels [14], and Cassidy and co-workers [17] concluded that there is a correlation between the ion abundances and the stoichiometry of the oxide. Experiments performed on chromium oxides by Muller and co-workers [18] demonstrated that the negative cluster ion distributions showed a good correlation with the stoichiometry of chromium in the oxides.

The main purpose of our experiments was to establish the compositions of the mentioned anions $[\text{M}_x\text{O}_y]^-$ and to examine their reactivity. It was found that the compositions of $[\text{M}_x\text{O}_y]^-$ anions formed by laser desorption ionisation are independent of the chemical composition of each metal oxide. Nevertheless the stoichiometry of the metal oxides could not be correlated with the ion intensities. As has been previ-

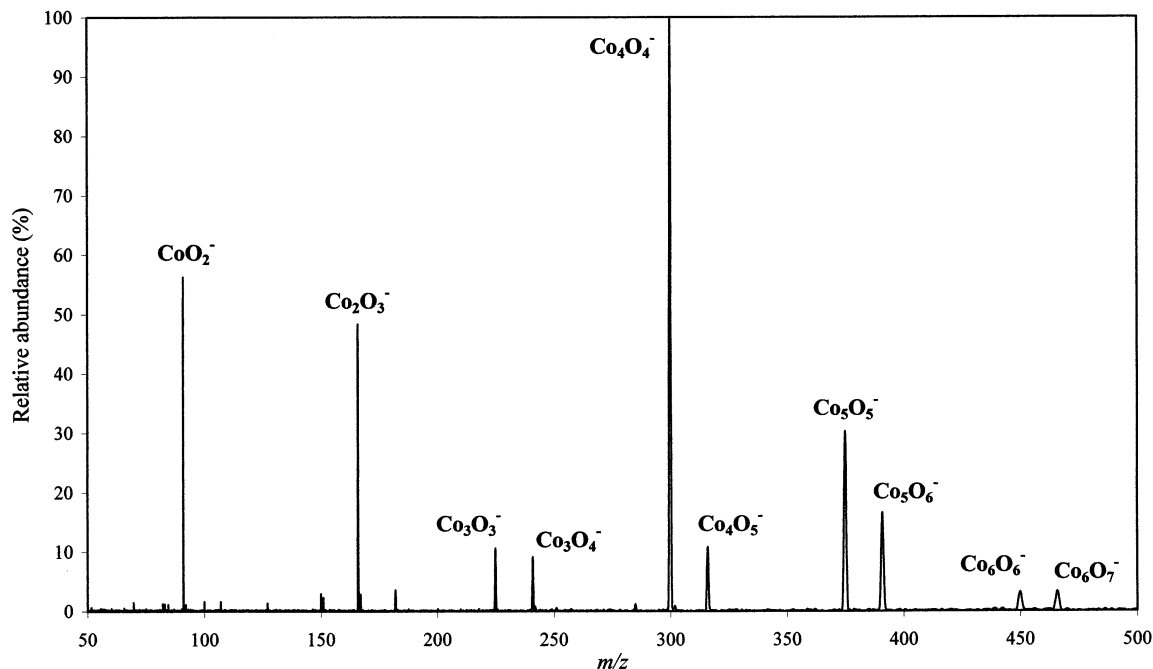


Fig. 1. Laser desorption ionisation negative ion mass spectrum of a Co_3O_4 pellet.

ously mentioned by other authors [17,18,35] it was observed that the intensity of the larger cluster anions increased as the laser power decreased. When the laser power is increased the intensity of small cluster anions increases and, in some cases, new small anions are also observed. In addition, some spectra such as those of the copper oxides show some distributions that only could be attributed to $[\text{M}_x\text{O}_y\text{H}_z]^-$ ions. These low abundant species can be originated either because of the presence of water adsorbed on the sample surface or the presence of hydroxyl groups on the metal oxide. Another possibility that cannot be excluded is that these species be formed in the laser plasma in consequence of the presence of residual water in the vacuum chamber of the instrument.

The compositions of observed anions, $([\text{M}_x\text{O}_y]^-; \text{M} = \text{Mn, Fe, Co, Ni, Cu})$ are displayed as ion maps. Fig. 2 shows plots of the number of oxygen atoms (y) versus the number of metal atoms (x), and the sizes of the circles indicate the relative intensities of the major negative cluster ions observed in the mass spectra. The ion maps of $[\text{Mn}_x\text{O}_y]^-$ show two dominant sets

of anions, one with $y = x + 1$ and the other with $y = x + 2$. It is also observed a lower intensity sequence with $y = x + 3$, for $x = 2$ and 3. The iron oxides yielded sequences of anions $[\text{Fe}_x\text{O}_{x+1}]^-$ and $[\text{Fe}_x\text{O}_{x+2}]^-$ for $x = 1 - 7$, and an additional series of $[\text{Fe}_x\text{O}_x]^-$, with $x = 3 - 5$. On the other hand, the maps of compositions for $[\text{Co}_x\text{O}_y]^-$ and $[\text{Ni}_x\text{O}_y]^-$ show series with $y = x$ and $y = x + 1$ as preferential distributions, while the $[\text{Cu}_x\text{O}_y]^-$ cluster anions predominantly belong to the oxygen-deficient class, that is, the spectrum is dominated by cluster ions that have a higher number of copper atoms than oxygen atoms although cluster anions with equivalent number of atoms of copper and oxygen were observed at lower masses. Similar distributions of anions $[\text{Cu}_x\text{O}_y]^-$ have been reported by Freiser and co-workers [16], but significant differences on the ion intensities could be observed. These authors found that the $[\text{Cu}_9\text{O}_6]^-$ cluster peak dominated the mass spectrum, while in our laser desorption ionisation mass spectra the most abundant peak was because of the bare copper anion.

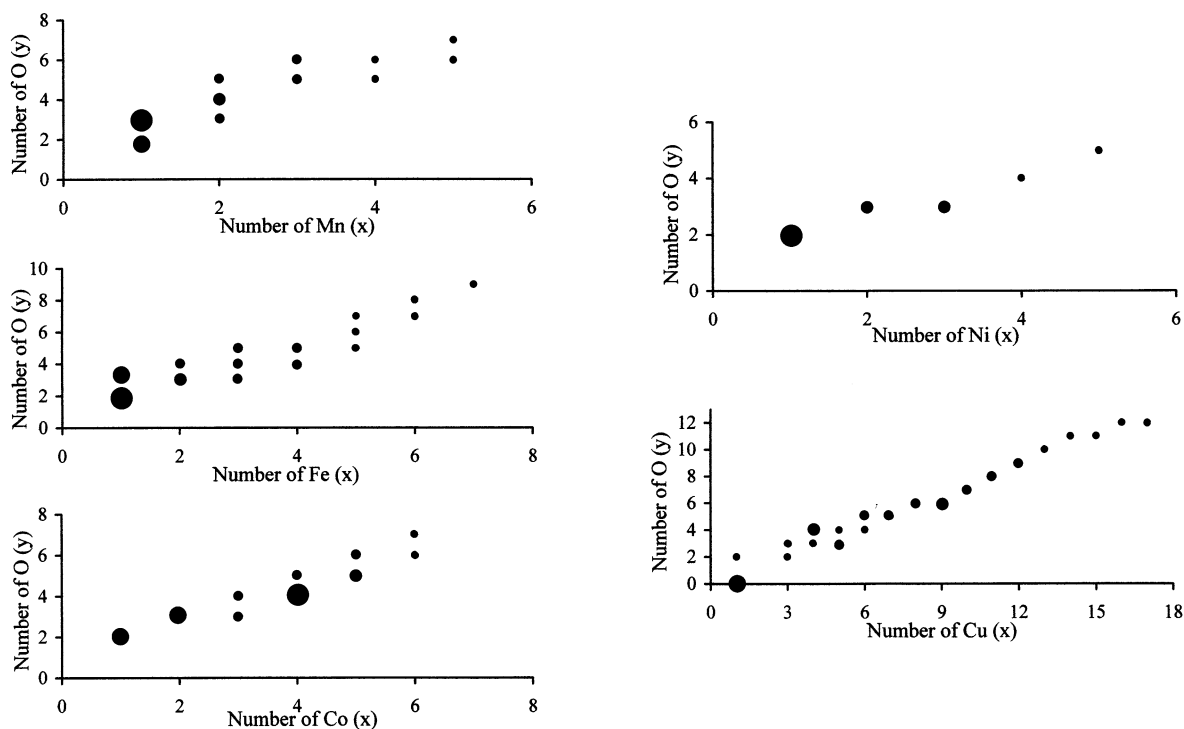


Fig. 2. Compositions and relative abundances of the $[\text{Mn}_x\text{O}_y]^-$, $[\text{Fe}_x\text{O}_y]^-$, $[\text{Co}_x\text{O}_y]^-$, $[\text{Ni}_x\text{O}_y]^-$, $[\text{Cu}_x\text{O}_y]^-$ ions. The sizes of the circles are approximately proportional to the ion intensities.

Although the sets of anions $[\text{M}_x\text{O}_y]^-$ seem to be independent of the composition of the solid sample, the distributions of compositions (x,y) seem to be related to the position of the metal in the transition-metal series. The fact that manganese exists in high oxidation states may explain the formation of oxygen-rich anions, while copper that prefers low oxidation states I and II yields predominantly oxygen-deficient negative ions, meaning that the metal to oxygen ratio increases as the electron population of the metal increases.

Valence electron population per metal atom, N_m , was evaluated by adding the number of $3d$ and $4s$ electrons of the neutral metal atom, plus six electrons for each atom of oxygen plus one electron because of the negative charge of the cluster, and dividing by the number of metal atoms in the cluster [32]. Table 1 shows calculated values of N_m for the $[\text{M}_x\text{O}_y]^-$ anions, allowing comparison of clusters with the same

numbers of metal atoms for Groups 7–11 of the Periodic Table. The most relevant observation is that the valence electron population per metal decreases as the size of the cluster increases, and in the larger cluster ions the normalised valence electron population tends to be independent of the type of the metal. According to Willet and coworkers [32,33] it could reflect the fact that for larger cluster anions the metal–metal bonding is strong in the core of the cluster, whilst at the external surface of the cluster predominates the oxygen–metal bonding.

To investigate if the cluster anions are desorbed directly from the solid or if they are formed in the plasma induced by the laser at the surface of the solid, a mixed-metal oxide and, for comparison, a mixture of two pure metal oxides were studied. The laser desorption ionisation spectrum of the mixed-metal oxide NiCo_2O_4 showed series of cluster anions of the type $[\text{Ni}_x\text{Co}_y\text{O}_z]^-$, with x or y varying between 0 and

Table 1
Valence electron population per metal atom, N_m , in $[M_xO_y]^-$ anions

Mn		Fe		Co		Ni		Cu	
Ion	N_m	Ion	N_m	Ion	N_m	Ion	N_m	Ion	N_m
MnO ₂	20.0	FeO ₂	21.0	CoO ₂	22.0	NiO ₂	23.0	CuO ₂	24.0
Mn ₂ O ₄	19.5	Fe ₂ O ₄	20.5	Co ₂ O ₄	21.5	Ni ₂ O ₃	19.5		
Mn ₃ O ₅	19.3	Fe ₃ O ₅	18.3	Co ₃ O ₄	17.3	Ni ₃ O ₃	16.3	Cu ₃ O ₃	17.3
Mn ₄ O ₅	14.8	Fe ₄ O ₅	15.8	Co ₄ O ₅	16.8	Ni ₄ O ₄	16.3	Cu ₄ O ₅	18.8
Mn ₅ O ₆	14.4	Fe ₅ O ₆	15.4	Co ₅ O ₆	16.4	Ni ₅ O ₅	16.2	Cu ₅ O ₄	16.0
		Fe ₆ O ₇	15.2	Co ₆ O ₇	16.2			Cu ₆ O ₅	16.2
		Fe ₇ O ₉	15.8					Cu ₇ O ₅	15.4
								Cu ₈ O ₆	15.6
								Cu ₉ O ₆	15.1
								Cu ₁₀ O ₇	15.3
								Cu ₁₁ O ₈	15.5
								Cu ₁₂ O ₉	15.7
								Cu ₁₃ O ₁₀	15.7
								Cu ₁₄ O ₁₁	15.8
								Cu ₁₅ O ₁₁	15.5
								Cu ₁₆ O ₁₂	15.9
								Cu ₁₇ O ₁₂	15.6

For $[M_xO_y]^-$, $N_m = [x (\text{number of } 3d \text{ and } 4s \text{ electrons in } M^0) + 6y + 1]/x$.

8, and z from 2 to 8, $[Co_4O_4]^-$ being the most intense anion. The 1.5:1 (w/w) mixture of NiO and Co_3O_4 oxides gave mostly $[Co_xO_y]^-$ anions, and in the region m/z 297–301 a distribution of peaks corresponding to $[Co_4O_4]^-$ and to a mixed-metal anion, probably $[NiCo_3O_4]^-$, was observed. The formation of a mixed nickel–cobalt anion when nickel oxide was mixed with cobalt oxide is in accordance with previous statements [33] that the clusters are assembled in the gas phase.

In order to have an insight of the structure of the $[M_xO_y]^-$ ions, collisionally-induced dissociation experiments with argon were performed. However, because of the loss of cluster ion intensity with increasing size, only the lower mass negative cluster ions could be isolated and studied by CID. The anions ($[M_xO_y]^-$; $x = 1, 2$; $y = 2, 3$), did not give any dissociation product ions. But, it was observed a decrease of its intensity with the increase of the collision energy, what may be explained assuming that the excited anions undergo a process of collisionally-induced electron detachment to form a neutral species with the same formula. Similar behaviour was observed on the collisionally-induced dissociations of some $[Mn_xS_y]^-$ [34] and $[Cu_xS_y]^-$ [33] cluster an-

ions as well as for several molybdenum oxide cluster anions [17].

3.2 Reactivity of transition metal oxide anions

The most intense transition metal anions described in the previous sections were isolated and their reactivity towards methanol was studied.

3.2.1. Monometallic oxide anions

The $([MO_2]^-; M = Mn, Fe, Co, Ni, Cu)$ anions react with methanol to yield $[MO_2H_2]^-$ as primary product, in accordance with Eq. (1)



The $[MO_2]^-$ anions cause the oxidative dehydrogenation of methanol into formaldehyde, an endothermic process ($\Delta H_r = 85.6 \text{ kJ mol}^{-1}$) (value determined for the reaction $CH_3OH \rightarrow CH_2O + H_2$ from available thermochemical data [36]). The reaction rate constants and the corresponding reaction efficiencies are reported in Table 2.

Rate constants, k_r , for the primary reactions of the $[MO_2]^-$ anions were calculated by plotting the natural

Table 2

Rate constant data for the primary reactions of $[\text{MO}_2]^-$ anions with methanol and *D*-labelled methanol

Ion	$k_{(\text{CH}_3\text{OH})}^{\text{a}}$	$k_{(\text{CH}_3\text{OD})}^{\text{a}}$	$k_{(\text{CD}_3\text{OH})}^{\text{a}}$	$k_{(\text{CD}_3\text{OD})}^{\text{a}}$	$k_{(\text{CH}_3\text{OH})}/k_{(\text{ADO})}$
$[\text{MnO}_2]^-$	2.7	0.9	0.9	1.6	0.12
$[\text{FeO}_2]^{-\text{b}}$	2.3	1.1	3.3	2.0	0.10
$[\text{CoO}_2]^-$	0.6	0.2	0.3	0.2	0.03
$[\text{NiO}_2]^-$	0.003	0.0001
$[\text{CuO}_2]^-$	0.001	0.000 08

^a Rate constants are reported in units of $10^{-10} \text{ cm}^3 \text{ mol}^{-1} \text{ s}^{-1}$.^b The rate constants were determined considering only the points which displayed a linear dependence of the natural logarithm of the abundance of the reactant vs time.

logarithm of relative abundance of the reactant ion versus time, at constant pressure. Laser desorption ionisation can produce ions that are kinetically or electronically excited [37]. However, semilog plots of $\log [\text{MO}_2]^-$ versus time displayed linear decay for all the anions studied (except for the iron dioxide anion) consistent with ions predominantly in the ground state. Moreover, the introduction of a thermalisation period in the reaction sequence using argon as colliding gas for the majority of the ions did not affect the rate constants or product distributions. For the anion $[\text{FeO}_2]^-$ no effective thermalisation was achieved even using collisional gases with higher cooling efficiencies, like xenon or methane. Consequently, only an approximate value for the rate constant of the reaction between the $[\text{FeO}_2]^-$ anion and methanol is given in Table 2.

As shown in Table 2 the reaction efficiencies decrease from $[\text{MnO}_2]^-$ to $[\text{CuO}_2]^-$, the $[\text{MnO}_2]^-$ and $[\text{FeO}_2]^-$ anions react with moderate efficiency with methanol ($k_r/k_{\text{ADO}} = 0.12$ and 0.10 , respectively), whereas the $[\text{CoO}_2]^-$, $[\text{NiO}_2]^-$, and $[\text{CuO}_2]^-$ anions show a lower reactivity towards methanol. Although the anions $[\text{NiO}_2]^-$ and $[\text{CuO}_2]^-$ react very slowly to form the primary products, it was possible to determine experimental rate constants because no competitive reactions between these anions and the background were observed.

The reactivity of the $[\text{MnO}_2]^-$, $[\text{FeO}_2]^-$, and $[\text{CoO}_2]^-$ ions with CH_3OD and CD_3OD was examined and the corresponding kinetic data are presented in Table 2. As referred in Sec. 2, CH_3OH and CD_3OH were present in the CH_3OD and CD_3OD samples with

average abundances of 40% and 15%, respectively, as measured by electron impact mass spectra recorded prior to the reactivity experiments. Consequently, rate constants for reactivity towards CD_3OH could also be calculated and presented in Table 2. The measured relative abundances were taken into account in the calculations of the rate constants. Reactions with CH_3OD and CD_3OH give rise to $[\text{MO}_2\text{HD}]^-$ products indicating that elimination of hydrogen atoms involves the hydroxyl and methyl groups of methanol. The reactions with the *D*-labelled compounds proceed more slowly than with methanol suggesting the occurrence of an isotope effect. The values of Table 2, however, do not allow us to infer any conclusions about reaction mechanisms, as there are no clear connections among the rate constants determined for the different *D*-labelled compounds.

In reaction (1) oxidation of methanol to formaldehyde is provided by the $[\text{MO}_2]^-$ anions, formally resulting in a charge transfer of two electrons from methanol to the metal atom. This process should result in a decrease of the formal oxidation state of the metal from +3 to +1 yielding $[\text{MO}_2\text{H}_2]^-$ products with a dihydroxide structure, like $[\text{M}(\text{OH})_2]^-$. Moreover, it is known that in transition metal oxides, the electronegativity of oxygen causes the metal to take on a Lewis acid character. If the metal acts as a Lewis acid in the anion, it is reasonable to consider that the reaction mechanism involves initial proton abstraction followed by hydride transfer from the alcohol to the metal centre yielding $[\text{H}(\text{MO})(\text{OH})]^-$ species. A mechanism similar to the latter one was proposed by Nibbering and co-workers [10] to account for the

reactions between $[\text{MnO}_2]^-$ and C_2 – C_4 primary alcohols.

The behaviour of primary product ions upon low-energy CID experiments was studied and no dissociation products were found. As observed previously for metal oxide anions, an electron detachment process may occur.

Few information about the electronic structures of transition-metal oxide anions is available. Mass spectrometric studies and ab initio calculations indicated that $[\text{FeO}_2]^-$ has an OFeO^- type of structure [13]. A photoelectron spectroscopy study of $[\text{FeO}_2]^-$ is also consistent with a stable $\text{O}=\text{Fe}=\text{O}$ bent structure, the oxidation state of Fe being + 3 [19,20]. In this formal oxidation state, the Fe atom has a stable d^5 configuration, although it was found that this anion reacts with methanol quite efficiently.

A photoelectron spectroscopy study of $[\text{CuO}_2]^-$ anions reported two distinct isomers: a species corresponding to the $\text{Cu}(\text{O}_2)$ complex and a dominant copper dioxide isomer [21]. The ground state of the CuOO anion is expected to be a closed shell structure with a $^1A''$ symmetry. The other isomer, probably with a $\text{O}^-\text{Cu}^{2+}\text{O}^-$ linear structure, should also have a closed shell $^1\Sigma_g^+$ ground state. This may explain the extremely low reactivity observed for the $[\text{CuO}_2]^-$ anions.

For the remaining anions no electronic structural data were found. However, it is expected that the dioxide structure can also be the more stable configuration of these anions. Although the decrease of the reactivity from the $[\text{FeO}_2]^-$ to $[\text{CuO}_2]^-$ can be correlated with the increasing number of electrons in the d shell along the first row of the transition metal series, only the assignment of the electronic configuration of the ground state of these anions would allow to interpret the behaviour of these species in the gas phase.

It was observed that for the monometallic anions of Mn, Fe, and Co (but not of Ni or Cu) the product formed according reaction (1) reacts further with methanol yielding a secondary product ion $[\text{MO}_3]^-$, as shown in Eq. (2)



The deuterated methanol experiments confirmed the formation of $[\text{MO}_3]^-$ as secondary products. These secondary reactions proceed with very low reaction efficiencies, 0.004 when $M = \text{Mn, Fe}$, and 0.0006 for Co.

As mentioned above, only the laser desorption ionisation of manganese and iron oxides produced $[\text{MO}_3]^-$ anions. The $[\text{MnO}_3]^-$ and $[\text{FeO}_3]^-$ were isolated and their reactivity toward methanol was investigated. No detectable product ions were obtained for reaction delays up to 10 s. Also, the $[\text{MO}_3]^-$ ions formed in the secondary reaction (2) did not react further with methanol to yield tertiary products, at longer reaction times. Published data show that the d^3 -trioxoiron (V) anion has a higher electron affinity than the d^5 -dioxoiron (III) anion [20], and a rather high Fe–O stretching frequency in FeO_3 suggesting that the Fe–O bonds are quite strong in this species. Although data for the manganese species are not available, higher electron affinities associated to higher oxidation states may explain the formation of very stable $[\text{MO}_3]^-$ anions.

It is worth noting that Nibbering and co-workers [10] found that the $[\text{MnO}_2]^-$ anion was unreactive towards methanol for reaction delay times up to 2 s, whereas the $[\text{MnO}_3]^-$ anion reacted with methanol to form ionic products. It was also found that the C_2 – C_4 primary alcohols are oxidised by the former anion to form a product ion identified by the authors as the $[\text{MnO.OH.H}]^-$. This different behaviour in the reactivity of the dioxomanganate (III) and trioxomanganate (V) anions when compared with the results reported in this article seems to be related to the process of preparation of the cluster ions. Nibbering synthesised the anions in the ICR cell by reactions of $[\text{Mn}(\text{CO})_x]^-$ with dioxygen, whilst in our study the clusters were generated by direct laser desorption ionisation of manganese oxide powders. As a consequence of the different ways of preparation, it is reasonable to assume that the gaseous ions may be formed in distinct electronic states, exhibiting different reactivities. On the other hand, in the latter case the oxometallate ion, a terminal product of a reaction between carbonyl metallate anions and dioxygen, can be formed by binding O_2 as a superoxo ligand [8,9]

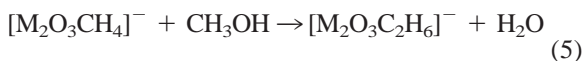
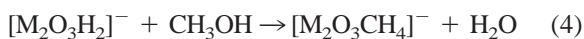
Table 3
Reaction efficiencies for the primary reactions of $[M_2O_3]^-$ anions with methanol

Ion	$k_{(CH_3OH)}/k_{ADO}$
$[Mn_2O_3]^-$	0.10
$[Fe_2O_3]^-$	0.17
$[Co_2O_3]^-$	0.09
$[Ni_2O_3]^-$	0.03

yielding an anion with distinct structural, physical and chemical properties.

3.2.2. Dimetallic oxide anions

The cluster anions, $[Mn_2O_3]^-$, $[Fe_2O_3]^-$, $[Co_2O_3]^-$, and $[Ni_2O_3]^-$ reacted with methanol with elimination of formaldehyde as primary process in accordance with Eq. (3). The overall reaction rate constants, k_r , and reaction efficiencies for the primary ion-molecule reaction of each cluster anion are shown in Table 3. For longer reaction times, the primary product reacts with other methanol molecules originating secondary products, depicted in sequences (4) and (5). The experiments with deuterated methanol confirmed that water elimination occurs in further reactions of the primary products.

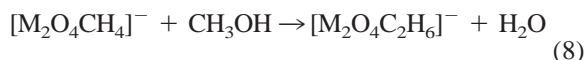
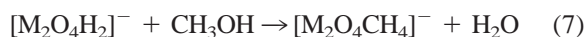


When the reactant is the manganese cluster $[Mn_2O_3]^-$, the reaction with methanol originates two products, the $[Mn_2O_3H_2]^-$ and another ion with m/z 31. The last seems to result of a proton abstraction of the substrate yielding the $[CH_3O]^-$ ion with loss of a neutral manganese specie $[Mn_2O_3H]$.

The primary products ($[M_2O_3H_2]^-$; M = Fe, Co) were collisionally activated with argon, and $[MO_2H]^-$ and neutral $[MOH]$ were formed. CID experiments on $[M_2O_3CH_4]^-$ products originated $[M_2O_3CH_2]^-$, $[M_2O_2H_2]^-$, and $[MO_2H_2]^-$ as ionic products accompanied by loss of neutral molecules, H_2 , CH_2O , and $[MCH_2O]$, respectively. The CID reactions of tertiary

products $[M_2O_3C_2H_6]^-$ yielded $[M_2O_2CH_4]^-$ and $[M_2O_2CH_2]^-$ as fragment ions with loss of CH_2O , and CH_3OH or CH_2O , H_2 molecules, respectively.

As observed previously with the other cluster anions, an oxidation of methanol occurs for the $[Mn_2O_4]^-$ and $[Fe_2O_4]^-$ anions yielding $[Mn_2O_4H_2]^-$ and $[Fe_2O_4H_2]^-$ as primary products. Both reactions have low kinetic efficiencies $k/k_{ADO} = 0.05$ and 0.04 , respectively. Each primary product reacts again with methanol and a secondary product is formed accompanied by water elimination. Subsequent reactions of the secondary products could also be observed. The occurrence of these reactions was established by means of the double-resonance technique. For both anions, the reaction sequences are summarised in Eqs. (6–8).



As found for the monometallic oxide anions, the bimetallic oxide anions react primarily with methanol via the elimination of aldehyde yielding ($[M_2O_yH_2]^-$, $y = 3$ or 4) products. Further reactions of the primary and secondary products with methanol are accompanied by water elimination suggesting that hydroxide ligands are involved. Consequently, ($[M_2O_y(OH)_2]^-$, $y = 1$ or 2) configurations could be proposed for the $[M_2O_3H_2]^-$ and $[M_2O_4H_2]^-$ primary products.

Scarce structural data are available for transition metal oxide clusters in the gas phase. The anion photoelectron spectrum reported by Wang and co-workers [20] for the Fe_2O_3 cluster suggests the presence of two isomeric Fe_2O-O_2 or Fe_2-O_3 complexes. The latter may have three bridging O atoms between the two Fe atoms in which the oxygen atoms are equivalent, while the former is consistent with a bend structure with an O-Fe-O-Fe-O atomic arrangement. Similar structures are found for the Cu_2O_3 anion [22]. It may be mentioned that a density functional calculation of geometrical and electronic structures of manganese sulfide cluster anions [38]

indicated that the Mn_2S_3 anion has a variety of possible structures, the most stable being a nonplanar structure with a Mn–Mn bond with an acute μ -S bridge, and two terminal Mn–S bonds. However, both the reactivity and the CID experimental results obtained in the present study could suggest a structure with two terminal M–O bonds for the bimetallic oxide anions, but thus not allow to conclude about the formation of metal–metal bonds.

It has been proposed [39] that the reactivity of a particular ionic cluster can be related with the degree of coordinative unsaturation in the metal ions. This quantity is evaluated from the electron deficiency (ED) per metal atom as given by the expression (9)

$$\text{ED} = [18 \times N - (\text{total no. of valence electrons})]/N \quad (9)$$

where N is the number of metal atoms in the cluster ion, the number of valence electrons being deduced from assumed structures. Assuming the structures proposed for the diiron oxide molecules [20], the electron deficiency of the $[\text{Fe}_2\text{O}_3]^-$ cluster anion can be evaluated considering eight valence electrons on each iron atom, plus four electrons for each oxygen ligand. Having in mind the negative charge on the cluster fragment, the electron deficiency for $[\text{Fe}_2\text{O}_3]^-$ would be 3.5. This value indicates that there are three open coordination sites on each iron atom. For the $[\text{Fe}_2\text{O}_4]^-$ cluster the calculated electron deficiency is only 1.5. Because the electron deficiency is an indication of the number of open coordination sites on a metal atom, it is expected that the relative reaction rate for the $[\text{Fe}_2\text{O}_4]^-$ should be lower than the reaction rate for the $[\text{Fe}_2\text{O}_3]^-$ cluster.

When calculating the electron deficiencies per metal atom for the different $[\text{M}_2\text{O}_3]^-$ dimetallic anions it was found that the number of open coordination sites in each metal atom decreases in the following order, $[\text{Mn}_2\text{O}_3]^- > [\text{Fe}_2\text{O}_3]^- > [\text{Co}_2\text{O}_3]^- > [\text{Ni}_2\text{O}_3]^-$, predicting that the reaction rates will decrease along first row of the transition metal series, what is consistent with the reaction efficiencies indicated in Table 3.

4. Conclusion

Laser desorption ionisation coupled with FTICR mass spectrometry was employed to generate and characterise a large number of transition metal oxide anions from powdered transition metal oxides. The sets of anions $([\text{M}_x\text{O}_y]^-; \text{M} = \text{Mn, Fe, Co, Ni, Cu})$ do not directly reflect the composition of the solid samples suggesting that the anions are formed in the laser induced plasma at the surface of the sample.

The more abundant anions $([\text{M}_x\text{O}_y]^-; x = 1 \text{ or } 2; y = 2, 3 \text{ or } 4)$ were isolated and their reactivity towards methanol was investigated. It was found that anions $[\text{MO}_2]^-$, $[\text{M}_2\text{O}_3]^-$ and $[\text{M}_2\text{O}_4]^-$ react primarily with methanol via the elimination of aldehyde yielding $[\text{M}_x\text{O}_y\text{H}_2]^-$ products, whereas the $[\text{MO}_3]^-$ anion did not react at all. The rate constants determined for the various reactions suggest that the $[\text{MO}_2]^-$ and $[\text{M}_2\text{O}_3]^-$ anions react more efficiently with methanol than the $[\text{M}_2\text{O}_4]^-$ cluster anion and on the other hand that reaction efficiencies decrease when the metal varies from manganese to copper.

Some more labelling experiments have to be performed and, in order to predict the geometrical structures, the electronic structures and the stabilities of $([\text{M}_x\text{O}_y]^-; \text{M} = \text{Mn, Fe, Co, Ni, Cu})$ cluster anions observed in the gas phase, molecular orbital calculations using the density functional theory (DFT) approach are in progress.

Acknowledgements

The authors are grateful to the Group of Inorganic Chemistry of the Faculty of Sciences of the University of Lisbon for the gift of the mixed metal oxide sample. This work was in part supported by a PRAXIS XXI project (contract no. PRAXIS/PCEX/C/QUI/72/96).

References

- [1] D. Schröder, H. Schwarz, *Angew. Chem. Int. Ed. Engl.* 34 (1995) 1973.
- [2] O. Gehret, M.P. Irion, *Chem. Eur. J.* 2 (1996) 598.

- [3] J.B. Griffin, P.B. Armentrout, *J. Chem. Phys.* 106 (1997) 4448.
- [4] E.F. Fialko, A.V. Kikhtenko, V.B. Goncharov, K.I. Zamaraev, *J. Phys. Chem. A* 101 (1997) 8607.
- [5] E.F. Fialko, A.V. Kikhtenko, V.B. Goncharov, K.I. Zamaraev, *J. Phys. Chem. B* 101 (1997) 5772.
- [6] E.F. Fialko, A.V. Kikhtenko, V.B. Goncharov, *Organometallics* 17 (1998) 25.
- [7] R.C. Bell, K.A. Zemski, K.P. Kerns, H.T. Deng, A.W. Castleman Jr., *J. Phys. Chem. A* 102 (1998) 1733.
- [8] K. Lane, L. Sallans, R.R. Squires, *J. Am. Chem. Soc.* 106 (1984) 2719.
- [9] R.R. Squires, *Chem. Rev.* 87 (1987) 623.
- [10] H. Fokkens, I.K. Gregor, N.M.M. Nibbering, *Rapid Commun. Mass Spectrom.* 5 (1991) 368.
- [11] S.W. Sigsworth, A.W. Castleman Jr., *J. Am. Chem. Soc.* 114 (1992) 10 477.
- [12] R.G. Keesee, B. Chen, A.C. Harms, A.W. Castleman Jr., *Int. J. Mass Spectrom. Ion Processes* 123 (1993) 225.
- [13] D. Schröder, A. Fiedler, J. Schwarz, H. Schwarz, *Inorg. Chem.* 33 (1994) 5094.
- [14] E. Michiels, R. Gijbels, *Spectrochim. Acta* 38B (1983) 1347.
- [15] E. Michiels, R. Gijbels, *Anal. Chem.* 56 (1984) 1115.
- [16] J.R. Gord, R.J. Bemish, B.S. Freiser, *Int. J. Mass Spectrom. Ion Processes* 102 (1990) 115.
- [17] C.J. Cassady, D.A. Weil, S.W. McElvany, *J. Chem. Phys.* 96 (1992) 691.
- [18] A. Hachimi, E. Poitevin, G. Krier, J.F. Muller, M.F. Ruiz-Lopes, *Int. J. Mass Spectrom. Ion Processes* 144 (1995) 23.
- [19] J. Fan, L-S. Wang, *J. Chem. Phys.* 102 (1995) 8714.
- [20] H. Wu, S.R. Desai, L-S. Wang, *J. Am. Chem. Soc.* 118 (1996) 5296.
- [21] H. Wu, S.R. Desai, L-S. Wang, *J. Chem. Phys.* 103 (1995) 4363.
- [22] L-S. Wang, H. Wu, S.R. Desai, L. Lou, *Phys. Rev. B* 53 (1996) 8028.
- [23] W.D. Vann, R.L. Wagner, A.W. Castleman Jr., *J. Phys. Chem. A* 102 (1998) 1708.
- [24] K. Poels, L. Van Vaeck, R. Gijbels, *Anal. Chem.* 70 (1998) 504.
- [25] H. Struyf, L. Van Vaeck, K. Poels, R. Van Grieken, *J. Am. Chem. Soc. Mass Spectrom.* 9 (1998) 482.
- [26] M.H. Mendonça, Ph.D. thesis, FCUL, Lisboa, 1993.
- [27] S. Guan, A.G. Marshall, *Int. J. Mass Spectrom. Ion Processes* 157/158 (1996) 5.
- [28] J. Marçalo, J.P. Leal, A. Pires de Matos, A.G. Marshall, *Organometallics* 16 (1997) 4581.
- [29] T. Su, M.T. Bowers, in *Gas Phase Ion Chemistry*, Vol 1, M.T. Bowers (Ed.), Academic, New York, 1979, p. 83.
- [30] *CRC Handbook of Chemistry and Physics*, 75th Ed., D.R. Lide (Ed.), CRC, Boca Raton, FL, 1994.
- [31] J. El Nakat, I.G. Dance, K.J. Fisher, D. Rice, G.D. Willet, *J. Am. Chem. Soc.* 113 (1991) 5141.
- [32] J. El Nakat, K.J. Fisher, I.G. Dance, G.D. Willet, *Inorg. Chem.* 32 (1993) 1931.
- [33] K.J. Fisher, I.G. Dance, G.D. Willet, M. Yi, *J. Chem. Soc. Dalton Trans.* (1996) 709.
- [34] I.G. Dance, K.J. Fisher, G.D. Willet, *J. Chem. Soc. Dalton Trans.* (1997) 2557.
- [35] M. Moini, J.R. Eyler, *Chem. Phys. Lett.* 137 (1987) 311.
- [36] S.G. Lias, J.E. Bartmess, J.F. Liebman, J.L. Holmes, R.D. Levin, W.G. Mallard, *J. Phys. Chem. Ref. Data* 17 (1988) (Suppl. 1).
- [37] H. Kang, J.L. Beauchamp, *J. Phys. Chem.* 89 (1985) 3364.
- [38] I.G. Dance, K.J. Fisher, *J. Chem. Soc. Dalton Trans.* (1997) 2563.
- [39] D.A. Fredeen, D.H. Russell, *J. Am. Chem. Soc.* 107 (1985) 3762.